Acta Geophysica (2021) 69:1611–1621
https://doi.org/10.1007/s11600-021-00630-5

RESEARCH ARTICLE - APPLIED GEOPHYSICS

A new acoustic traveltime approximation for attenuating transversely isotropic media

Han Xiao[1] · **Deli Wang**[1]

Received: 28 February 2021 / Accepted: 8 June 2021 / Published online: 12 July 2021

Abstract
Attenuation is one of the most important quantities in describing seismic wave propagation, which is also anisotropic because of the dispersion relationship between the seismic wave and the symmetry direction. Transverse isotropic media with titled symmetry-axis (TTI) is a widespread approximation of the Earth's surface. For 2D TTI attenuating media, we firstly use the acoustic assumption to simplify the exact eikonal equation for the complex-valued quasi P-wave traveltime. Then we design a perturbation method to obtain the new approximation by solving the acoustic attenuating eikonal equation of TTI media and use Shanks transform to increase precision. Compared with former studies, the new approximation considers the symmetry-axis angles of the media as a factor, which will improve its robustness. The approximation is tested in several medium to demonstrate its effectiveness. The energy velocity which derived by the steepest-descent method is used to calculate the exact complex-valued traveltime. We test the accuracy of the approximations developed with and without Shanks transform in the following. Finally, we discussed the possibility to apply this approximation to the methods like fast marching methods.

Keywords Attenuation · TTI · Acoustic · Perturbation · Shanks transform

Introduction

The wave propagation in the layers of Earth subsurface can be better described by considering the medium to be anisotropic. Specially, a transverse isotropic (TI) media with symmetry-axis normal to the layering could be more efficient to represent big parts of the subsurface (Audubert et al. 2006; Alkhalifah and Sava 2010). In many applications, developing simple traveltime formulations for such models is of great significance.

Modeling the attenuating nature of the earth becomes more and more important because we need a closer look at amplitude for inversion purposes during analysis of recorded data. In attenuating media, seismic wave propagation is different from that in elastic media. The value of traveltime of time-harmonic wave is complex, and the complex-valued traveltime is governed by the complex-valued eikonal equation (Červený and Pšenčík 2009). The real and imaginary parts of the complex-valued traveltime, respectively, correspond to the phase of the waves and the waves' amplitude decay caused by energy absorption. The inversion approaches of Q filtering naturally use the imaginary part of the complex-valued traveltime. Besides, in other techniques such as attenuation tomography and Kirchhoff migration, the complex-valued traveltime is also a fundamental component.

By means of similar principles to the real ray-tracing methods, the complex ray tracing methods have been developed for anelastic anisotropic media (e.g., Zhu and Chun 1994; Thomson 1997; Chapman et al. 1999; Kravtsov et al. 1999; Hangya and Seredynska 2000; Amodei et al. 2006). The complex ray theory can exactly solve the complex-valued eikonal equation, and it is hardly affected by the strength of anisotropy and attenuation of the media (Vavryčuk 2010). But in realistic 3D models, the complex ray theory is difficult to accomplish because the model parameters cannot be extended into complex space. To implement the complex ray tracing in practice, researchers (Gajewski and Pšenčík 1992; Červený 2001; Červený and Pšenčík 2009; Klimeš and Klimeš 2011) developed the perturbation method to calculate the complex-valued traveltimes of body waves in attenuating media approximately by setting the imaginary

Communicated by Prof. Sanyi Yuan.

✉ Han Xiao
xiaohan15@mails.jlu.edu.cn

[1] College of Geo-Exploration Science and Technology, Jilin University, Changchun, China

parts of complex-valued stiffness coefficients as the perturbation parameters. In perturbation methods, wave attenuation is presumed to be weak and similar to the nonattenuating reference medium, the complex-valued traveltimes are calculated along the real ray path. Therefore, the perturbation methods are simpler and more efficient than the complex ray tracing method. Without considering strongly attenuating media, the perturbation methods are more suitable for realistic models. By perturbation theory, Hao and Alkhalifah (2017a, b) developed an approximate method to solve the acoustic eikonal equation for attenuating transversely isotropic media with vertical symmetry-axis (VTI). For TI media with known symmetry-axis angle, Hao and Alkhalifah's approximation could work with a simple transformation. However, if the symmetry-axis angle is unknown, the approximation will certainly suffer from this limitation.

Besides, finite-difference methods (e.g., Vidale 1988, 1990), fast sweeping methods (e.g., Zhang et al. 2006; Luo and Qian 2012), fast marching methods (e.g., Sethian 1996; Vladimirsky 2001; Alkhalifah 2011) and many other methods related to solve the eikonal equation by spatial discretization have been applied in nonattenuating isotropic media. General obstacles of these methods are solving the eikonal equation and selecting the minimum of traveltime in the heap to update the traveltime in the grids along the direction of wave front expansion. These methods have high computational efficiency but in attenuating media, it's not valid to select the minimum complex-valued traveltime. For this reason, these methods involved in solving the eikonal equation directly have been limited to nonattenuating media.

In this paper, we develop an approximate method to solve the acoustic eikonal equation for attenuating transversely isotropic media with titled symmetry-axis (TTI) under the assumption that the symmetry of velocity and attenuation is same. We adopt the Thomsen's (1986) and Zhu and Tsvankin's (2006) notations as well as the symmetry-axis angle to parameterize the media (see "Appendix 1"). Besides, we also combine the Vogit's notation to describe the symmetry-axis directions. We simplify the eikonal equation by setting $V_{s0}=0$ and $A_{s0}=0$, which is called acoustic approximation. The acoustic eikonal equation for attenuating TTI media contains two nonlinear partial differential equations correspond to the real and imaginary parts of the traveltime, respectively. We adopt these parameters to characterize the acoustic eikonal equation: the vertical velocity v_{p0}, the anellipticity parameter η, the vertical attenuation coefficient A_{p0}, the attenuation anisotropy parameters ε_Q and δ_Q and the NMO velocity v_n. We design a perturbation method to approximately calculate the complex-valued traveltime. In the second-order Taylor series expansion consisting of the parameters η, ik and $sin\theta$ (here k is calculated by the parameter A_{p0}, which is mentioned in the following text), we obtain several equations which are related to the partial derivative of these parameters. In the case of homogeneous media, we can get the complex-valued traveltime by solving these equations analytically. To find results with higher accuracy, we apply two different Shanks transforms to the Taylor series solution.

At the same time, the parameterization in the perturbation method also allows us to proceed in inhomogeneous media. For the complex part of traveltimes is divided by the parameter ik, we don't need to select the minimum value from complex-valued traveltimes. At the end of the paper, we discuss a fast marching method based on this approximation.

The exact eikonal equation

As is stated by Ben-Menahem and Singh (1981) and Carcione (2015), wavefield-modeling methods could expand to attenuation by using the complex-valued stiffness coefficients to substitute the real-valued stiffness coefficients. In attenuating media, Voigt notated frequency-domain stiffness coefficients c_{ij}, which are real-valued in nonattenuating media are expressed by (Červený and Pšenčík 2005, 2009):

$$c_{ij} = c_{ij}^R - \mathrm{i}c_{ij}^I. \tag{1}$$

In this equation, the letter i is the imaginary unit, the elements c_{ij}^R and c_{ij}^I denote the real and imaginary parts of c_{ij}. As to nonattenuating media, the imaginary part of c_{ij} becomes zero. The symbol "−" is due to the minus sign in the exponential element $\exp(-\mathrm{i}\omega t)$ considering the time-harmonic wave (Červený and Pšenčík 2009), where t is the time, and ω is the angular frequency. For nonattenuating anisotropic media, the c_{ij} matrix is a positive definite matrix, because the strain energy is always positive (Fedorov 1968; Carcione 2015). For a time-domain harmonic plane wave in an attenuating anisotropic media which is described by the exponential factor $\exp(-\mathrm{i}\omega t)$, the c_{ij}^R and c_{ij}^I matrices are also positive definite (Červený and Pšenčík 2006), which is a descendent of the positive strain energy and the dissipat energy.

According to Eq. 1, (Gajewski and Pšenčík 1992; Vavryčuk 2007, 2010) obtained the zeroth-order time-domain harmonic ray solution described by the particle displacement vector:

$$\boldsymbol{u}(\boldsymbol{x}, t) = \boldsymbol{U}(\boldsymbol{x})\exp(-\mathrm{i}\omega(t - \tau(\boldsymbol{x}))). \tag{2}$$

In this equation, $\boldsymbol{x}$ is the position vector; t and ω denote the same vector as in the exponential element $\exp(-\mathrm{i}\omega t)$; $\boldsymbol{U}(\boldsymbol{x})$ is the element that affects wave amplitude along the ray path, and its direction is identical to the displacement vector $\boldsymbol{u}(\boldsymbol{x}, t)$; $\tau = \tau_R + \mathrm{i}\tau_I$ denotes the complex-valued traveltime of rays.

We can rewrite the exponential term $exp(-\mathrm{i}\omega(t - \tau(\boldsymbol{x})))$ in Eq. 2 to the form:

$$\exp(-\mathrm{i}\omega(t - \tau(\boldsymbol{x}))) = \exp(-\mathrm{i}\omega(t - \tau_R(\boldsymbol{x})))\exp(-\omega\tau_I(\boldsymbol{x})). \tag{3}$$

In this equation, the element $exp(-i\omega\tau_I(\boldsymbol{x}))$ denotes the attenuation of wave amplitude. In accordance with Eq. 1, the positive and negative of τ_I are the same as ω. For positive ω, τ_I must always be positive which corresponds to the stiffness coefficients defined in Eq. 1, and for negative ω, τ_I must always be negative, which corresponds to the stiffness coefficients described by the complex conjugate of Eq. 1 (Hao and Alkhalifah 2017a). In attenuating isotropic media, this condition is similar to that the quasi *P*- and *S*-waves' quality factors are odd functions of angular frequency ω (Aki and Richards 2002).

In attenuating anisotropic media, we substitute Eq. 2 into the elastic-dynamic equation and obtain the Christoffel equation (Vavryčuk 2007) of quasi *P*- and *S*- waves for 2D VTI media, which is given by:

$$\begin{pmatrix} a_{11}p_1^2 + a_{55}p_3^2 - 1 & (a_{13}+a_{55})p_1p_3 \\ (a_{13}+a_{55})p_1p_3 & a_{55}p_1^2 + a_{33}p_3^2 - 1 \end{pmatrix}\begin{pmatrix} g_1 \\ g_3 \end{pmatrix} = 0. \quad (4)$$

In this equation, $a_{ij} = c_{ij}/\rho$ denote stiffness coefficients normalized by the density of the media, where c_{ij} has the same definition as the c_{ij} in Eq. 1, and ρ is the density of the media. In attenuating anisotropic media, we can define a_{ij} by using Thomsen's (1986) parameters and Zhu and Tsvankin's (2006) parameters in "Appendix 1"; g_1 is the horizontal directional polarization components; and g_3 is the vertical directional polarization components;p_1 is the horizontal directional slowness components, and p_3 is the vertical directional slowness components. We can rewrite p_1 and p_3 as the spatial derivative of the complex-valued traveltime of rays in time–space domain:

$$p_1 = \frac{\partial\tau}{\partial x},\ p_3 = \frac{\partial\tau}{\partial z}. \quad (5)$$

Using the rewritten forms of p_1 and p_3 in Eq. 4, we obtain the traveltime function of 2D attenuating VTI media described by the first order nonlinear partial differential in the *x*–*z* dimension:

$$\left(a_{11}\left(\frac{\partial\tau}{\partial x}\right)^2 + a_{55}\left(\frac{\partial\tau}{\partial z}\right)^2 - 1\right)\left(a_{55}\left(\frac{\partial\tau}{\partial x}\right)^2 + a_{33}\left(\frac{\partial\tau}{\partial z}\right)^2 - 1\right) - (a_{13}+a_{55})^2\left(\frac{\partial\tau}{\partial x}\right)^2\left(\frac{\partial\tau}{\partial z}\right)^2 = 0. \quad (6)$$

The structure of this equation is similar to that in nonattenuating VTI media. When it comes to 3D attenuating VTI media, we can replace the partial differential $\left(\frac{\partial\tau}{\partial x}\right)^2$ by the factor $\left(\left(\frac{\partial\tau}{\partial x}\right)^2 + \left(\frac{\partial\tau}{\partial y}\right)^2\right)$.

When it comes to TTI media, $\frac{\partial\tau}{\partial x}$ and $\frac{\partial\tau}{\partial z}$ in Eq. 6 are taken in the tilt direction. To get the eikonal equation for a 3D TTI medium, the partial differential in Eq. 6 should be rotated with the rotation matrix:

$$\begin{pmatrix} \cos\varphi\cos\theta & \sin\varphi\cos\theta & \sin\theta \\ -\sin\varphi & \cos\varphi & 0 \\ -\cos\varphi\sin\theta & -\sin\varphi\sin\theta & \cos\theta \end{pmatrix}. \quad (7)$$

Here,θ is the angle of the symmetry-axis measured from the vertical, and φ is the angle of the azimuth of the vertical plane (Alkhalifah 2011). In a 2D TTI medium, the azimuth of the vertical plane φ is zero, we can get the eikonal equation in *x*–*z* dimension:

$$\left(a_{11}\left(\cos\theta\frac{\partial\tau}{\partial x} + \sin\theta\frac{\partial\tau}{\partial z}\right)^2 + a_{55}\left(\cos\theta\frac{\partial\tau}{\partial z} - \sin\theta\frac{\partial\tau}{\partial x}\right)^2 - 1\right)\left(a_{55}\left(\cos\theta\frac{\partial\tau}{\partial x} + \sin\theta\frac{\partial\tau}{\partial z}\right)^2 + a_{33}\left(\cos\theta\frac{\partial\tau}{\partial z} - \sin\theta\frac{\partial\tau}{\partial x}\right)^2 - 1\right) - (a_{13}+a_{55})^2\left(\cos\theta\frac{\partial\tau}{\partial x} + \sin\theta\frac{\partial\tau}{\partial z}\right)^2\left(\cos\theta\frac{\partial\tau}{\partial z} - \sin\theta\frac{\partial\tau}{\partial x}\right)^2 = 0. \quad (8)$$

Equation 8 governs the complex P and SV wave traveltimes of 2D TTI media by density-normalized stiffness coefficients as well as directional slowness components. In order to solve Eq. 8, we will replace the complex density-normalized stiffness coefficients by several widespread parameters and rewrite this equation in the following.

The acoustic eikonal equation

For the acoustic eikonal equation of nonattenuating TI media, there is an approximation that the S-wave velocity v_{s0} has little influence on the quasi P-wave velocity. That is called the "acoustic approximation" (Hao and Alkhalifah 2017a). When it comes to attenuating anisotropic media, a similar approximation is defined such that the S-wave attenuation coefficient A_{s0} also doesn't affect the P-wave attenuation coefficient much (Zhu and Tsvankin 2006). According to the acoustic approximation, we can set $v_{s0} = 0$ and $A_{s0} = 0$, and then we use Alkhalifah's (1998, 2000) parameters $v_{p0}, v_n = v_{p0}\sqrt{1+2\delta}, \eta = (\varepsilon-\delta)/(1+2\delta)$ to describe the nonattenuating reference media (see Eqs. 26 and 27 in "Appendix 1" and use Zhu and Tsvankin's (2006) notation A_{p0}, ε_Q, δ_Q to describe the attenuation part. A_{p0} describes the decay of displacement amplitude per wavelength, ε_Q and δ_Q describe the anisotropy for the media's attenuation. A_{p0} is normalized by the corresponding wavenumber, which is defined as the number of radians in a unit distance. The 2D acoustic attenuating TTI eikonal equation is given by:

$$A\left(\cos\theta\frac{\partial\tau}{\partial x}+\sin\theta\frac{\partial\tau}{\partial z}\right)^2+B\left(\cos\theta\frac{\partial\tau}{\partial z}-\sin\theta\frac{\partial\tau}{\partial x}\right)^2 +C\left(\cos\theta\frac{\partial\tau}{\partial x}+\sin\theta\frac{\partial\tau}{\partial z}\right)^2\left(\cos\theta\frac{\partial\tau}{\partial z}-\sin\theta\frac{\partial\tau}{\partial x}\right)^2=1, \tag{9}$$

in which A, B and C, respectively, correspond to:

$$A=v_n^2(1+2\eta)\left(1-2ik\left(1+\varepsilon_Q\right)\right) \tag{10}$$

$$B=v_{p0}^2(1-2ik) \tag{11}$$

$$C=\frac{v_{p0}^2}{v_n^2}((1-2ik)v_n^2-ik\delta_Q v_{p0}^2)^2-v_{p0}^2v_n^2(1+2\eta)(1-2ik)\left(1-2ik\left(1+\varepsilon_Q\right)\right), \tag{12}$$

with:

$$k=\frac{A_{p0}}{1-A_{p0}^2}. \tag{13}$$

Equation 9 with Eqs. 10–13 is the acoustic eikonal equation for 2D TTI attenuating media. Solving Eq. 9 numerically requires solving a quartic equation at each computational step, which will bring huge computational cost. As an alternative, we can use perturbation theory to solve Eq. 9 by approximating it with a series of simpler linear equations. Considering η,k and θ constant and small, we can represent the traveltime solution as a series expansion in η,k and θ.

The analytical solution for homogeneous media

We set a trial solution to the Eq. 9 by perturbation method for homogeneous media:

$$\tau=\tau_0+\sum_{i=1}^{3}\tau_i l_i+\sum_{i,j=1;i\le j}^{3}\tau_{ij}l_i l_j \tag{14}$$

$$l=(\eta,\mathrm{i}k,sin\theta)^T. \tag{15}$$

Equation 14 is an expansion in terms of the attenuation anisotropy parameters in Eq. 15. By inserting this equation into Eq. 9, we obtain a second-order expansion of the eikonal equation with the respect to the parameters in Eq. 15. On the basis of that all the coefficients of the same parameters must equal zero, we could derive several equations to govern the traveltime coefficients:

$$v_n^2\left(\frac{\partial\tau_0}{\partial x}\right)^2+v_{p0}^2\left(\frac{\partial\tau_0}{\partial z}\right)^2=1 \tag{16}$$

$$v_n^2\frac{\partial\tau_0}{\partial x}\frac{\partial\tau_i}{\partial x}+v_{p0}^2\frac{\partial\tau_0}{\partial z}\frac{\partial\tau_i}{\partial z}=f_i(\tau_0),\quad i=1,\ 2,3, \tag{17}$$

$$v_n^2\frac{\partial\tau_0}{\partial x}\frac{\partial\tau_{ij}}{\partial x}+v_{p0}^2\frac{\partial\tau_0}{\partial z}\frac{\partial\tau_{ij}}{\partial z}=f_{ij}(\tau_0,\tau_1,\tau_2,\tau_3),\quad i=1,2,3,\ \text{and}\ \ i\le j. \tag{18}$$

Equations 16–18, respectively, represent the zeroth-, first-, and second-order traveltime coefficients.

Solving Eq. 16, we can get that:

$$\tau_0=\frac{\sqrt{(v_{p0}^2x^2+v_n^2z^2)}}{v_nv_{p0}}. \tag{19}$$

Then with the result in Eq. 19, we can evaluate $\frac{\partial\tau_0}{\partial x}$ and $\frac{\partial\tau_0}{\partial z}$ and insert them into Eq. 17 to calculate τ_i(i = 1,2,3). Using the same method, we can get τ_{ij}(i = 1,2,3, and i ≤ j) by solving Eq. 18. With the solutions obtained by Eqs. 17 and 18, we can calculate the approximate traveltime in Eq. 14. The right-hand-sides of Eqs. 17–18 are shown in "Appendix 2", and their solutions are shown in "Appendix 3".

Bender and Orszag (1978) produced a method to improve the convergence rate of a sequence of partial sums (or of any sequence for that matter) by eliminating its most pronounced transient behavior, which is called Shanks transform. In this approximation, it could be applied on the traveltime coefficients to get the approximation further improved. We designed two Shanks transform solutions in Eqs. 20 and 21:

$$\tau=\tau_0+\frac{(\tau_1\eta+\mathrm{i}\tau_2k+\tau_3sin\theta)^2}{\tau_1\eta+\tau_3sin\theta-\tau_{11}\eta^2-\tau_{13}\eta sin\theta-\tau_{22}k^2-\tau_{33}sin^2\theta+\mathrm{i}(\tau_2k-\tau_{12}\eta k-\tau_{23}ksin\theta)}, \tag{20}$$

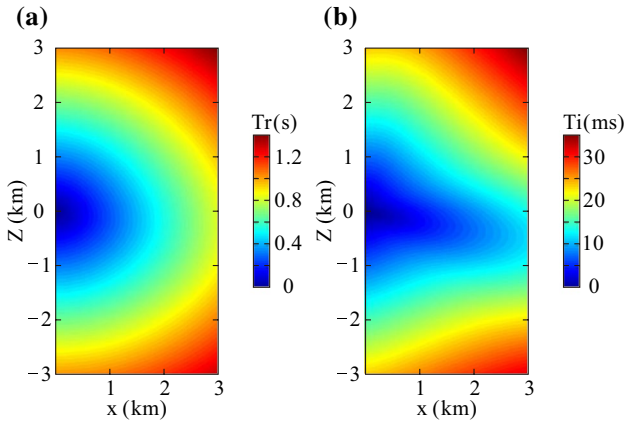

Fig. 1 The real (**a**) and the imaginary (**b**) part of the complex-valued traveltime for TTI medium whose azimuth angle is 10°

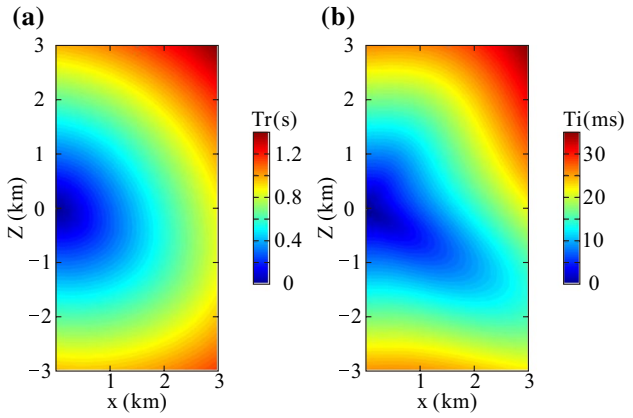

Fig. 2 The real (**a**) and the imaginary (**b**) part of the complex-valued traveltime for TTI medium whose azimuth angle is 30°

$$\tau = \tau_0 + \mathrm{i}\tau_2 k - \tau_{22}k^2 + \frac{\left(\tau_1\eta + \mathrm{i}\tau_{12}\eta k + \mathrm{i}\tau_{23}ksin\theta\right)^2}{\tau_1\eta - \tau_{11}\eta^2 - \tau_{13}\eta sin\theta - \tau_{33}sin\theta^2 + \mathrm{i}(\tau_{12}\eta k + \tau_{23}ksin\theta)}. \quad (21)$$

Equations 20 and 21 could reduce to the approximate traveltime for simpler media on some special condition. When we set all the perturbation parameters to zero, then $\tau = \tau_0$, Eqs. 20 and 21 will reduce to the traveltime equation for isotropic VTI media. When we set $k = 0$, Eqs. 20 and 21 will reduce to the traveltime equation for nonattenuating TTI media, which is the same as Alkhalifah (2011). When we set $sin\theta = 0$, Eqs. 20 and 21 will reduce to the traveltime equation for attenuating VTI media (Hao and Alkhalifah 2017a).

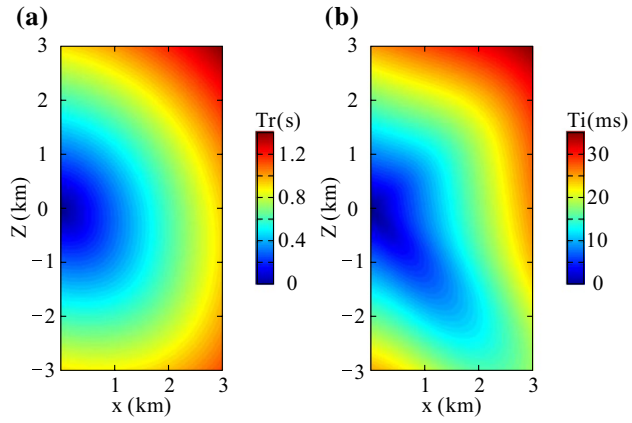

Fig. 3 The real (**a**) and the imaginary (**b**) part of the complex-valued traveltime for TTI media whose azimuth angle is 50°

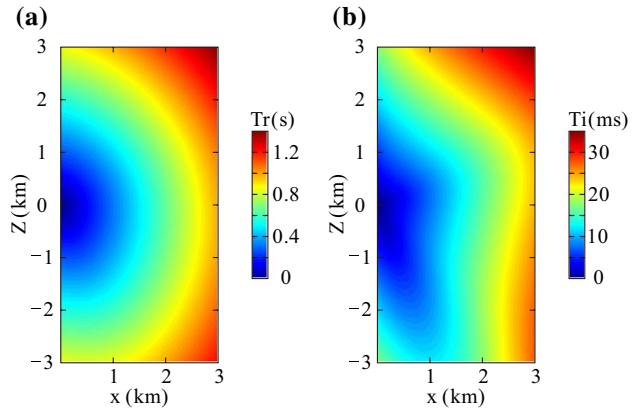

Fig. 4 The real (**a**) and the imaginary (**b**) part of the complex-valued traveltime for TTI media whose azimuth angle is 70°

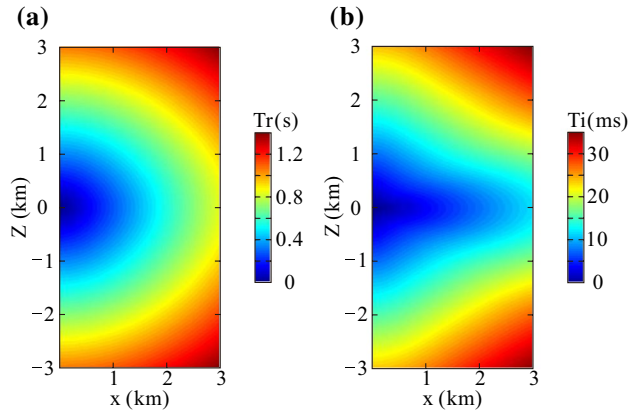

Fig. 5 The real (**a**) and the imaginary (**b**) part of the complex-valued traveltime for VTI media

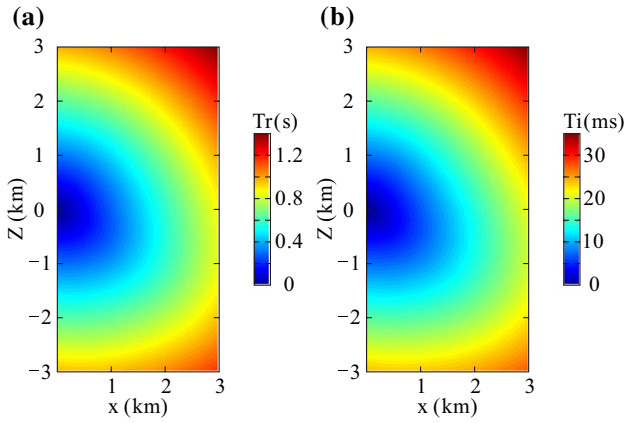

Fig. 6 The real (**a**) and the imaginary (**b**) part of the complex-valued traveltime for media with isotropic attenuation

Examples

In this part, we firstly demonstrate the effectiveness of Eq. 14 with the results in "Appendix 3". Figures 1, 2, 3 and 4 show the real part as well as the imaginary part of the complex-valued traveltimes for TTI medium with different azimuth angles. Figure 5 shows the complex-valued traveltimes for VTI media with the same anisotropic parameter as Fig. 1. Figure 6 shows the traveltimes for a TTI media whose attenuation is isotropic. The model parameters of the tested models are listed in Table 1. The attenuation parameters in Table 1 are derived from Zhu and Tsvankin (2006).

From Figs. 1, 2, 3 and 4, we can see the symmetry axes of the isochrons perfectly meet the symmetry axes of the corresponding models. It is worth to mention that even when the azimuth angle of the model is 70°, which couldn't be regarded as small, the Eq. 14 with the results in "Appendix 3" works smoothly. From Figs. 1, 2, 3 and 4, we can obtain that the attenuation anisotropy performed stronger than the wave propagation anisotropy. In Figs. 1a to 4a, the traveltime along the azimuth's direction is smaller than the traveltime along the direction perpendicular to the azimuth, because the P-wave velocity along the azimuth's direction v_{p0} is larger than the NMO velocity v_n. This could also be proved by the following result in VTI media. From Figs. 1b to 4b, we can find that the shape of the isochrons is different to the corresponding real part, which is caused by the anisotropic of the attenuation. We will use a same media with isotropic attenuation to verify this finding.

In Fig. 5, we could clearly see the traveltimes along different directions are different, which is caused by the different between v_{p0} and v_n. The real and imaginary part of the complex-valued traveltime in Fig. 4 is also the same as the result in Hao and Alkhalifah (2017a).

Compare Figs. 6b and 2b, we can see when the attenuation of the media is isotropic, the shape of the imaginary traveltime's isochron is the same as the real traveltime's isochron. The anisotropic of attenuation has obviously influence on the imaginary traveltime. However, the isochron in Fig. 6a, compared with that in Fig. 2a, doesn't have much difference, which indicate that the changes on attenuation parameters have little influence to the real traveltime.

After demonstrating the effectiveness, we will test the accuracy of the approximate traveltime Eq. 14 in the following. The exact traveltime to be compared is calculated by the propagating distance, and the complex-valued energy velocity calculated by Vavryčuk (2007). Figure 7 shows the real part as well as the imaginary part of the exact complex-valued traveltime. The model parameters of Fig. 7 are the same as Fig. 2, which could be found in Table 1.

We could see little difference between the isochron in Fig. 7 and Fig. 2 that means the approximate traveltime Eq. 14 has reliable accuracy. We will use Eqs. 22 and 23 to calculate the absolute errors of the real part and the imaginary part of the complex-valued traveltime:

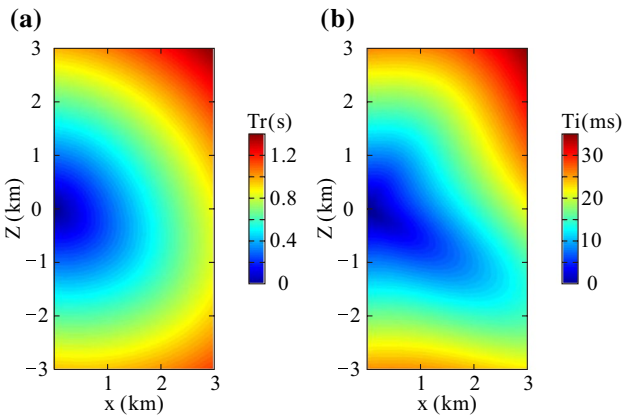

Fig. 7 The real (**a**) and the imaginary (**b**) part of the exact complex-valued traveltime

Table 1 Model parameters of the numerical model

	v_n(km/s)	v_{p0}(km/s)	η	ε_Q	δ_Q	θ
Figures 1, 2, 3 and 4	3	3.286	0.167	−0.33	0.98	10°, 30°, 50°, 70°
Figure 5	3	3.286	0.167	−0.33	0.98	0°
Figure 6	3	3.286	0.167	0	0	30°

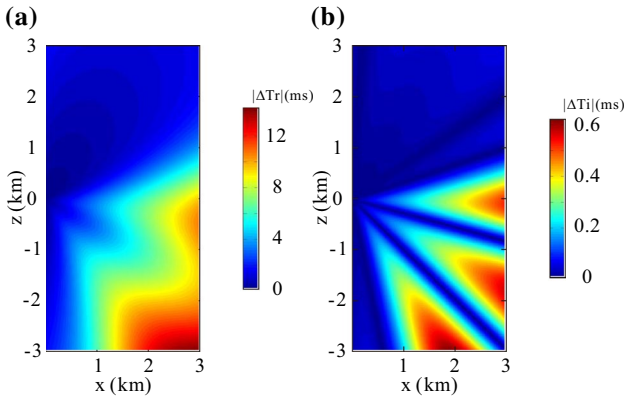

Fig. 8 Absolute errors in the real (**a**) and imaginary (**b**) part of the complex-valued traveltime calculated by Eq. 14

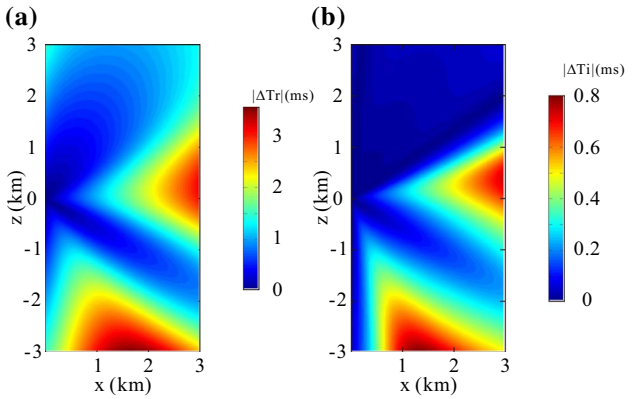

Fig. 9 Absolute errors in the real (**a**) and imaginary (**b**) part of the complex-valued traveltime calculated by Eq. 20

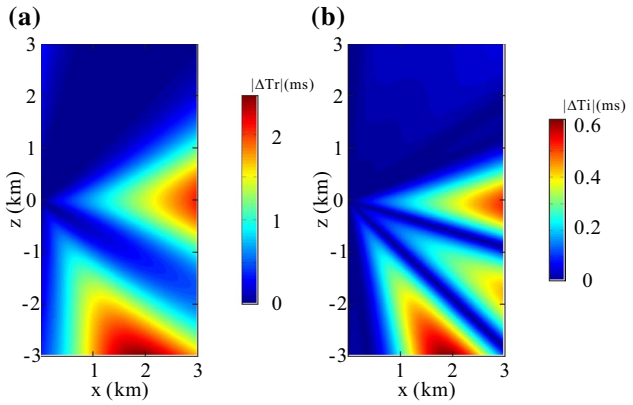

Fig. 10 Absolute errors in the real (**a**) and imaginary (**b**) part of the complex-valued traveltime calculated by Eq. 21

Table 2 Error evaluation

/	Average	Maximum	Percentage (%)
$\lvert\Delta T_r\rvert$	3.41	13.31	0.4
$\lvert\Delta T_i\rvert$	0.32	1.52	1.85

Table 3 Error evaluation with Equation 20

/	Average	Maximum	Percentage (%)
ΔT_r	0.66	2.53	0.1
ΔT_i	0.09	0.38	0.5

Table 4 Error evaluation with Equation 21

/	Average	Maximum	Percentage (%)
ΔT_r	0.68	2.56	0.1
ΔT_i	0.14	0.61	0.4

$$\left|\Delta T_r(x,z)\right| = \left|T_r^{\mathrm{cal}}(x,z) - T_r^{\mathrm{ex}}(x,z)\right|, \tag{22}$$

$$\left|\Delta T_i(x,z)\right| = \left|T_i^{\mathrm{cal}}(x,z) - T_i^{\mathrm{ex}}(x,z)\right|. \tag{23}$$

Here, x and z represent the horizontal and vertical axis of the tested model, ΔT_r and ΔT_i are the absolute errors in the real and imaginary parts of the complex-valued traveltime. T_r^{ex} and T_i^{ex} are the real and imaginary parts of the exact complex-valued traveltime as shown in Fig. 7. T_r^{cal} and T_i^{cal} are the real and imaginary parts of the complex-valued traveltime calculated by the approximate traveltime equations, in Fig. 8, they are calculated by Eq. 14 and in Figs. 9 and 10, they are calculated by Eqs. 20 and 21.

We evaluate the accuracy by the average value, the maximum value and the percentage error. The error data are listed in Table 2.

The average value is about a quarter of the maximum, so the errors are more distributed in small values. The percentage error of T_r is acceptable, and the percentage error of T_i need to be improved.

We also evaluate the accuracy by the average value, the maximum value and the percentage error. The error data for Fig. 9 are listed in Table 3.

From the data listed in Table 3, we can obtain that there is no singular value appears, so the application of Shanks transform doesn't reduce the stability. From the updated error data in Table 2, the maximum value and the percentage error are greatly reduced, and the errors are still more distributed in small values, the accuracy has been improved.

From the error data in Fig. 10 and Table 4, we can find that the maximum value and the percentage error is similar

to that in Fig. 9 and Table 3. Compare with the isochrons in Fig. 9, the real part of the absolute error in Fig. 10 is smaller on the direction perpendicular to the inclination. At the same time, the imaginary part of the absolute error in Fig. 10 is relatively larger on the incline direction. We could choose between Eqs. 20 and 21 according to the practical needs in the application.

Discussion

Besides perturbation theory, we could also solve the approximation eikonal equation by spatial discretization methods. With all the real items in Eqs. 16, 17 and 18, we are able to select the minimum traveltime in the real and imaginary part, respectively, which provides probability to use the methods like finite-difference methods (e.g., Vidale, 1988, 1990), fast sweeping methods (e.g., Zhang et al., 2006; Luo and Qian, 2012) and fast marching methods in attenuating media. As an example, we would discuss a fast marching scheme to calculate the two-point traveltime numerically.

First, we evaluate the zeroth-order traveltime coeffcient τ_0. The fast marching method (Sethian, 1996; Alkhalifah, 2011) is implemented to solve Eq. 16 numerically. Second, we evaluate the first- and second-order traveltime coeffcients τ_i and τ_{ij} by solving Eqs. 17 and 18 successively in the order of calculating τ_0 in the fast marching method.

With τ_0, τ_i and τ_{ij} evaluated, the Shanks transform is also valid to improve the accuracy of the traveltime in fast marching method. As we see in the 'Numerical examples' section, the Shanks transform solution 2 (Eq. 21) is most accurate among all of the proposed traveltime solutions for a homogeneous attenuating TTI medium. Hence, we could evaluate the traveltime τ from the Shanks transform solution 21.

Conclusion

We obtain an acoustic eikonal equation describes the complex-valued traveltime in attenuation anisotropy TTI media. This eikonal equation is derived on the basis that the S-wave parameters (includes Thomsen's notation v_{s0} and Zhu and Tsvankin's notation A_{s0}) have little affection on the traveltime of P-wave in attenuation anisotropy TTI media. We use perturbation method to solve the acoustic eikonal equation and use Shanks transform to improve the accuracy of the solutions for homogeneous attenuation anisotropy TTI media. Numerical tests show that the solution of the acoustic eikonal equation could work smoothly in TTI medium with different azimuth angles. We demonstrate the influence of azimuth angle and anisotropic attenuation by VTI media and isotropic attenuation media. We test the accuracy of the solution of the acoustic eikonal equation. Finally, we discuss a fast marching scheme according to the approximation.

Appendix 1

Parameters' definition of attenuating TI media

In this part, we further define the parameters for attenuation TI media to match the calculation process of traveltime. These parameters are all defined with stiffness coefficients c_{ij}, quality factors Q_{ij} and density ρ. The stiffness coefficients are described in Eq. 1. The quality factors matrix is $Q_{ij} = c_{ij}^R / c_{ij}^I$.

(1) v_{p0}: P-wave's velocity when propagating along the z-axis,

$$v_{p0} \equiv \sqrt{\frac{c_{33}^R}{\rho}}. \tag{24}$$

(2) v_{s0}: S-wave's velocity when propagating along the z-axis,

$$v_{p0} \equiv \sqrt{\frac{c_{55}^R}{\rho}}. \tag{25}$$

(3) ϵ, δ, γ: The nonattenuating Thomsen's (1986) parameters,

$$\epsilon \equiv \frac{c_{11}^R - c_{33}^R}{2c_{33}^R} \tag{26}$$

$$\delta \equiv \frac{(c_{13}^R + c_{55}^R)^2 - (c_{33}^R - c_{55}^R)^2}{2c_{33}^R(c_{33}^R - c_{55}^R)} \tag{27}$$

$$\gamma \equiv \frac{c_{66}^R - c_{55}^R}{2c_{55}^R}. \tag{28}$$

(4) A_{p0}: P-wave attenuation coefficients along the z-axis,

$$A_{p0} \equiv Q_{33}\left(\sqrt{1 + \frac{1}{Q_{33}^2}} - 1\right). \tag{29}$$

(5) A_{s0}: S-wave attenuation coefficients along the z-axis,

$$A_{s0} \equiv Q_{55}\left(\sqrt{1+\frac{1}{Q_{55}^2}}-1\right). \tag{30}$$

(6) $\varepsilon_Q, \delta_Q, \gamma_Q$: The attenuating Thomsen-type parameters,

$$\varepsilon_Q \equiv \frac{Q_{33}-Q_{11}}{Q_{11}} \tag{31}$$

$$\delta_Q \equiv \frac{\frac{Q_{33}-Q_{55}}{Q_{55}} c_{55}^R \frac{(c_{13}^R+c_{33}^R)^2}{(c_{33}^R-c_{55}^R)} + 2\frac{Q_{33}-Q_{13}}{Q_{13}} c_{13}^R (c_{13}^R+c_{55}^R)}{c_{33}^R (c_{33}^R-c_{55}^R)} \tag{32}$$

$$\gamma_Q \equiv \frac{Q_{55}-Q_{66}}{Q_{66}}. \tag{33}$$

Equations 24–28 are from Thomsen's (1986) and mainly describe the real part of the complex-valued traveltime. Equations 29–33 are from Zhu and Tsvankin (2006) and describe the imaginary part of the complex-valued traveltime.

Appendix 2

The right-hand-side of the equations 17 and 18

By inserting Eq. 14 into Eq. 9, we obtain a second-order expansion of the eikonal equation with the respect to the parameters in Eq. 15. On the basis of that all the coefficients of the same parameters must equal zero, we could derive the right-hand-side of the Eqs. 17 and 18.

The right-hand-side of the Eq. 17 are:

$$f_1(\tau_0) = -v_n^2\left(\frac{\partial \tau_0}{\partial x}\right)^2 + v_{p0}^2 v_n^2 \left(\frac{\partial \tau_0}{\partial x}\right)^2 \left(\frac{\partial \tau_0}{\partial z}\right)^2 \tag{34}$$

$$f_2(\tau_0) = 1 + v_{p0}^4 \delta_Q v_n^2 \left(\frac{\partial \tau_0}{\partial x}\right)^2 \left(\frac{\partial \tau_0}{\partial z}\right)^2 + \varepsilon_Q \left(1 - v_{p0}^2 \left(\frac{\partial \tau_0}{\partial z}\right)^2\right)^2 \tag{35}$$

$$f_3(\tau_0) = \left(v_n^2 - v_{p0}^2\right)\left(\frac{\partial \tau_0}{\partial x}\right)\left(\frac{\partial \tau_0}{\partial z}\right). \tag{36}$$

The functions in the right-hand-side of Eq. 18 are:

$$\begin{aligned} f_{11}(\tau_0,\tau_1) = {} & -2v_n^2 \frac{\partial \tau_0}{\partial x}\frac{\partial \tau_1}{\partial x} + 2v_{p0}^2 v_n^2 \frac{\partial \tau_0}{\partial x}\left(\frac{\partial \tau_0}{\partial z}\right)^2 \frac{\partial \tau_1}{\partial x} \\ & + 2v_{p0}^2 v_n^2 \left(\frac{\partial \tau_0}{\partial x}\right)^2 \frac{\partial \tau_0}{\partial z}\frac{\partial \tau_1}{\partial z} - \frac{1}{2}v_n^2\left(\frac{\partial \tau_1}{\partial x}\right)^2 - \frac{1}{2}v_{p0}^2\left(\frac{\partial \tau_1}{\partial z}\right)^2 \end{aligned} \tag{37}$$

$$\begin{aligned} f_{22}(\tau_0,\tau_2) = {} & -\frac{1}{2}v_n^2\left(\frac{\partial \tau_2}{\partial z}\right)^2 + 2v_n^2(1+\varepsilon_Q)\frac{\partial \tau_0}{\partial x}\frac{\partial \tau_2}{\partial x} - \frac{1}{2}v_{p0}^2\left(\frac{\partial \tau_2}{\partial z}\right)^2 \\ & + 2v_{p0}^2 \frac{\partial \tau_0}{\partial z}\frac{\partial \tau_2}{\partial z} + 2v_{p0}^4 \delta_Q \frac{\partial \tau_0}{\partial x}\frac{\partial \tau_0}{\partial z}\left(\frac{\partial \tau_2}{\partial x}\frac{\partial \tau_0}{\partial z} + \frac{\partial \tau_0}{\partial x}\frac{\partial \tau_2}{\partial z}\right) \\ & - 2v_{p0}^4 \delta_Q \left(\frac{\partial \tau_0}{\partial x}\right)^2\left(\frac{\partial \tau_0}{\partial z}\right)^2 - \frac{v_{p0}^6}{2v_n^2}\delta_Q^2\left(\frac{\partial \tau_0}{\partial x}\right)^2\left(\frac{\partial \tau_0}{\partial z}\right)^2 \\ & - 2v_n^2 v_{p0}^2 \varepsilon_Q \frac{\partial \tau_0}{\partial x}\frac{\partial \tau_0}{\partial z}\left(\frac{\partial \tau_2}{\partial x}\frac{\partial \tau_0}{\partial z} + \frac{\partial \tau_0}{\partial x}\frac{\partial \tau_2}{\partial z}\right) \\ & + 2v_n^2 v_{p0}^2 \varepsilon_Q \left(\frac{\partial \tau_0}{\partial x}\right)^2\left(\frac{\partial \tau_0}{\partial z}\right)^2 \end{aligned} \tag{38}$$

$$\begin{aligned} f_{33}(\tau_0,\tau_3) = {} & v_{p0}^2 - v_n^2\left(\frac{\partial \tau_3}{\partial x}\right)\left(\frac{\partial \tau_0}{\partial z}\right) - v_{p0}^2 - v_n^2\left(\frac{\partial \tau_0}{\partial x}\right)\left(\frac{\partial \tau_3}{\partial z}\right) \\ & + \frac{1}{2}\left(v_{p0}^2\left(\frac{\partial \tau_0}{\partial x}\right)^2 - v_{p0}^2\left(\frac{\partial \tau_3}{\partial x}\right)^2 - v_n^2\left(\frac{\partial \tau_0}{\partial x}\right)^2\right. \\ & \left. - v_n^2\left(\frac{\partial \tau_3}{\partial x}\right)^2 - \left(v_{p0}^2 - v_n^2\right)\left(\frac{\partial \tau_0}{\partial z}\right)^2\right) \end{aligned} \tag{39}$$

$$\begin{aligned} f_{12}(\tau_0,\tau_1,\tau_2) = {} & -v_n^2 \frac{\partial \tau_1}{\partial x}\frac{\partial \tau_2}{\partial x} + 2v_n^2(1+\varepsilon_Q)\frac{\partial \tau_0}{\partial x}\frac{\partial \tau_1}{\partial x} - 2v_n^2 \frac{\partial \tau_0}{\partial x}\frac{\partial \tau_2}{\partial x} \\ & + 2v_n^2(1+\varepsilon_Q)\left(\frac{\partial \tau_0}{\partial x}\right)^2 - v_{p0}^2 \frac{\partial \tau_1}{\partial z}\frac{\partial \tau_2}{\partial z} + 2v_{p0}^2 \frac{\partial \tau_0}{\partial z}\frac{\partial \tau_1}{\partial z} \\ & + 2v_{p0}^4 \delta_Q \frac{\partial \tau_0}{\partial x}\frac{\partial \tau_0}{\partial z}\left(\frac{\partial \tau_1}{\partial x}\frac{\partial \tau_0}{\partial z} + \frac{\partial \tau_0}{\partial x}\frac{\partial \tau_1}{\partial z}\right) \\ & - 2v_n^2 v_{p0}^2 \varepsilon_Q \frac{\partial \tau_0}{\partial x}\frac{\partial \tau_0}{\partial z}\left(\frac{\partial \tau_1}{\partial x}\frac{\partial \tau_0}{\partial z} + \frac{\partial \tau_0}{\partial x}\frac{\partial \tau_1}{\partial z}\right) \\ & + 2v_n^2 v_{p0}^2 \frac{\partial \tau_0}{\partial x}\frac{\partial \tau_0}{\partial z}\left(\frac{\partial \tau_2}{\partial x}\frac{\partial \tau_0}{\partial z} + \frac{\partial \tau_0}{\partial x}\frac{\partial \tau_2}{\partial z}\right) \\ & - 2v_n^2 v_{p0}^2 (2+\varepsilon_Q)\left(\frac{\partial \tau_0}{\partial x}\right)^2\left(\frac{\partial \tau_0}{\partial z}\right)^2 \end{aligned} \tag{40}$$

$$\begin{aligned} & f_{13}(\tau_0,\tau_1,\tau_3) \\ & = 2v_{p0}^2 v_n^2 \frac{\partial \tau_0}{\partial x}\frac{\partial \tau_0}{\partial z}\left(\frac{\partial \tau_0}{\partial z}\left(\frac{\partial \tau_3}{\partial x} + \frac{\partial \tau_0}{\partial z}\right) + \frac{\partial \tau_0}{\partial x}\left(\frac{\partial \tau_3}{\partial z} + \frac{\partial \tau_0}{\partial x}\right)\right) \\ & - v_n^2 \frac{\partial \tau_0}{\partial x}\frac{\partial \tau_3}{\partial z} - 2v_n^2 \frac{\partial \tau_0}{\partial x}\left(\frac{\partial \tau_3}{\partial x} + \frac{\partial \tau_0}{\partial z}\right) \\ & - v_n^2 \frac{\partial \tau_1}{\partial x}\left(\frac{\partial \tau_3}{\partial x} + \frac{\partial \tau_0}{\partial z}\right) + v_{p0}^2 \frac{\partial \tau_1}{\partial x}\frac{\partial \tau_0}{\partial z} \\ & - v_{p0}^2 \frac{\partial \tau_1}{\partial z}\left(\frac{\partial \tau_3}{\partial z} + \frac{\partial \tau_0}{\partial x}\right) \end{aligned} \tag{41}$$

$$
\begin{aligned}
&f_{23}(\tau_0,\tau_2,\tau_3)\\
&\quad=-v_n^2\frac{\partial\tau_2}{\partial x}\frac{\partial\tau_3}{\partial x}+2v_n^2(1+\varepsilon_Q)\frac{\partial\tau_0}{\partial x}\frac{\partial\tau_3}{\partial x}-v_{p0}^2\frac{\partial\tau_2}{\partial z}\frac{\partial\tau_3}{\partial z}\\
&\quad+2v_{p0}^2\frac{\partial\tau_0}{\partial z}\frac{\partial\tau_3}{\partial z}+2v_{p0}^4\delta_Q\frac{\partial\tau_0}{\partial x}\frac{\partial\tau_0}{\partial z}\left(\frac{\partial\tau_3}{\partial x}\frac{\partial\tau_0}{\partial z}+\frac{\partial\tau_0}{\partial x}\frac{\partial\tau_3}{\partial z}\right)\\
&\quad-2v_n^2v_{p0}^2\varepsilon_Q\frac{\partial\tau_0}{\partial x}\frac{\partial\tau_0}{\partial z}\left(\frac{\partial\tau_3}{\partial x}\frac{\partial\tau_0}{\partial z}+\frac{\partial\tau_0}{\partial x}\frac{\partial\tau_3}{\partial z}\right).
\end{aligned}
\tag{42}
$$

Appendix 3

The analytical solutions for homogeneous attenuating TI media

The analytical solution to Eq. 16 is:

$$
\tau_0=\frac{\sqrt{\left(v_{p0}^2x^2+v_n^2z^2\right)}}{v_nv_{p0}}.
\tag{43}
$$

The analytical solutions to Eq. 17 are:

$$
\tau_1=-\frac{x^4v_{p0}^3}{v_n\left(v_{p0}^2x^2+v_n^2z^2\right)^{3/2}},
\tag{44}
$$

$$
\tau_2=-\frac{v_{p0}^4\delta_Qx^2z^2+v_{p0}^4(1+\varepsilon_Q)x^4+2v_n^2v_{p0}^2x^2z^2+2v_n^4z^4}{v_nv_{p0}\left(v_{p0}^2x^2+v_n^2z^2\right)^{3/2}},
\tag{45}
$$

$$
\tau_3=\frac{\left(v_{p0}^2-v_n^2\right)xz}{\left(v_{p0}^2x^2+v_n^2z^2\right)}.
\tag{46}
$$

The analytical solutions to Eq. 18 are:

$$
\tau_{11}=\frac{3x^6v_{p0}^5\left(v_{p0}^2x^2+4v_n^2z^2\right)}{2v_n\left(v_{p0}^2x^2+v_n^2z^2\right)^{7/2}},
\tag{47}
$$

$$
\begin{aligned}
\tau_{22}=&-\frac{3v_{p0}\delta_Q^2x^2z^2\left(x^4v_{p0}^8-x^2z^2v_n^2v_{p0}^6+z^4v_n^4v_{p0}^4\right)}{2v_n^3\left(v_{p0}^2x^2+v_n^2z^2\right)^{7/2}}+\frac{3\delta_Qx^2z^2\left(1-\varepsilon_Qx^4v_{p0}^8+2(1+\varepsilon_Q)x^2z^2v_n^2v_{p0}^6+z^4v_n^4v_{p0}^4\right)}{2v_nv_{p0}\left(v_{p0}^2x^2+v_n^2z^2\right)^{7/2}}\\
&+3\frac{(1+\varepsilon_Q)^2x^8v_{p0}^8+4\left(1+\varepsilon_Q+\varepsilon_Q^2\right)x^6z^2v_n^2v_{p0}^6+2(3+\varepsilon_Q)x^4z^4v_n^4v_{p0}^4+x^2z^6v_n^6v_{p0}^2+z^8v_n^8}{2v_nv_{p0}\left(v_{p0}^2x^2+v_n^2z^2\right)^{7/2}}
\end{aligned}
\tag{48}
$$

$$
\tau_{33}=-\frac{3\left(v_{p0}^4x^4-v_{p0}^2v_n^2\left(x^4+z^4\right)+v_n^4z^4\right)}{2v_nv_{p0}\left(v_{p0}^2x^2+v_n^2z^2\right)^{5/2}}
\tag{49}
$$

$$
\tau_{12}=-\frac{x^4\left(v_nv_{p0}^7(1+\varepsilon_Q)x^4-3v_nv_{p0}^7x^2z^2+2v_n^3v_{p0}^5(1+4\varepsilon_Q)x^2z^2+6v_n^3v_{p0}^5\delta_Qz^4+(1-2\varepsilon_Q)v_n^5v_{p0}^3z^4\right)}{\left(v_{p0}^2x^2+v_n^2z^2\right)^{7/2}}
\tag{50}
$$

$$\tau_{13} = \frac{x^3 z v_{p0}^4 (3v_{p0}^2 x^2 + v_n^2 x^2 + 4v_n^2 z^2)}{v_n (v_{p0}^2 x^2 + v_n^2 z^2)^{5/2}} \tag{51}$$

$$\tau_{23} = \frac{3x^3 z \left(v_n v_{p0}^7 (1+\varepsilon_Q) x^4 - 3 v_n v_{p0}^7 x^2 z^2 + v_n^3 v_{p0}^5 \delta_Q z^4 + 4 v_n^5 v_{p0}^3 \varepsilon_Q z^4 \right)}{2 \left(v_{p0}^2 x^2 + v_n^2 z^2 \right)^{7/2}}. \tag{52}$$

Acknowledgements This work was supported by the Major Projects of the National Science and Technology of China (Grant No. 2016ZX05026-002-003) and the National Natural Science Foundation of China (41374108).

Declarations

Conflict of interest The author declares that there is no conflict of interest.

References

Aki K, Richards PG (2002) Quantitative seismology, 2nd edn. University Science Books

Alkhalifah T (1998) Acoustic approximations for seismic processing in transversely isotropic media. Geophysics 63:623–631. https://doi.org/10.1190/1.1444361

Alkhalifah T (2000) An acoustic wave equation for anisotropic media. Geophysics 65:1239–1250. https://doi.org/10.1190/1.1444815

Alkhalifah T (2011) Scanning anisotropy parameters in complex media. Geophysics 76(2):U13–U22. https://doi.org/10.1190/1.3553015

Alkhalifah T & Sava P (2010) Migration velocity analysis using a transversely isotropic medium with tilt normal to the reflector dip. Eage Conference and Exhibition - Workshops and Fieldtrips

Amodei D, Keers H, Vasco W, Johnson L (2006) Computation of uniform wave forms using complex rays. Phys Rev E 73:1–14

Audebert F, Pettenati A, and Dirks V (2006) Tti anisotropic depth migration-which tilt estimate should we use? In: 68th EAGE conference and exhibition incorporating SPE EUROPEC 2006

Bender CM, Orszag SA (1978) Advanced mathematical methods for scientists and engineers. McGraw-Hill

Ben-Menahem A, Singh SJ (1981) Seismic waves and sources. Springer

Carcione JM (2015) Wave fields in real media: Theory and numerical simulation of wave propagation in anisotropic, anelastic, porous and electromagnetic media: Handbook of Geophysical exploration, 3rd edn. Elsevier

Červený V (2001) Seismic ray theory. Cambridge University Press, Cambridge

Červený V, Pšenčík I (2005) Plane waves in viscoelastic anisotropic media—I. Theory. Geophys J Int 161:197–212. https://doi.org/10.1111/j.1365-246X.2005.02589.x

Červený V, Pšenčík I (2006) Energy flux in viscoelastic anisotropic media. Geophys J Int 166:1299–1317. https://doi.org/10.1111/j.1365-246X.2006.03057.x

Červený V, Pšenčík I (2009) Perturbation Hamiltonians in heterogeneous anisotropic weakly dissipative media. Geophys J Int 178:939–949. https://doi.org/10.1111/j.1365-246X.2009.04218.x

Chapman SJ, Lawry JMH, Ockendon JR, Tew RH (1999) On the theory of complex rays. SIAM Rev 41:417–509. https://doi.org/10.1137/S0036144599352058

Fedorov FI (1968) Theory of elastic waves in crystals. Springer

Gajewski D, Pšenčík I (1992) Vector wavefields for weakly attenuating anisotropic media by the ray method. Geophysics 57:27–38. https://doi.org/10.1190/1.1443186

Hanyga A, Seredyńska M (2000) Ray tracing in elastic and viscoelastic media. Pure Appl Geophys 157:679–717. https://doi.org/10.1007/PL00001114

Hao Q, Alkhalifah T (2017a) An acoustic eikonal equation for attenuating orthorhombic media. Geophysics 82:WA67–WA81

Hao Q, Alkhalifah T (2017b) An acoustic eikonal equation for attenuating transversely isotropic media with a vertical symmetry axis. Geophysics 82:C9–C20

Klimeš M, Klimeš L (2011) Perturbation expansion of complex-valued traveltime along real-valued reference rays. Geophys J Int 186:751–759. https://doi.org/10.1111/j.1365-246X.2011.05054.x

Kravtsov YA, Forbes GW, Asatryan AA (1999) Theory and applications of complex rays. In: Wolf E (ed) Progress in optics, pp. 1–62. Elsevier

Luo S, Qian J (2012) Fast sweeping methods for factored anisotropic eikonal equations: multiplicative and additive factors. J Sci Comput 52:360–382. https://doi.org/10.1007/s10915-011-9550-y

Sethian JA (1996) A fast marching level set method for monotonically advancing fronts. Proc Natl Acad Sci USA 93:1591–1595. https://doi.org/10.1073/pnas.93.4.1591

Sethian JA, Vladimirsky A (2001) Ordered upwind methods for static Hamilton–Jacobi equations. Proc Natl Acad Sci 98:11069–11074. https://doi.org/10.1073/pnas.201222998

Thomsen L (1986) Weak elastic anisotropy. Geophysics 51:1954–1966. https://doi.org/10.1190/1.1442051

Thomson CJ (1997) Complex rays and wave packets for decaying signals in inhomogeneous, anisotropic and anelastic media. Stud Geophys Geod 41:345–381. https://doi.org/10.1023/A:1023359401107

Vavryčuk V (2007) Ray velocity and ray attenuation in homogeneous anisotropic viscoelastic media. Geophysics 72(6):D119–D127. https://doi.org/10.1190/1.2768402

Vavryčuk V (2010) Behavior of rays at interfaces in anisotropic viscoelastic media. Geophys J Int 181:1665–1677

Vidale JE (1988) Finite-difference calculation of travel times. Bull Seismol Soc Am 78:2062–2076

Vidale JE (1990) Finite-difference calculation of traveltimes in three dimensions. Geophysics 55:521–526. https://doi.org/10.1190/1.1442863

Zhang Y-T, Zhao H-K, Qian J (2006) High order fast sweeping methods for static Hamilton–Jacobi equations. J Sci Comput 29:25–56. https://doi.org/10.1007/s10915-005-9014-3

Zhu TF, Chun KY (1994) Complex rays in elastic and anelastic media. Geophys J Int 119:269–276. https://doi.org/10.1111/j.1365-246X.1994.tb00927.x

Zhu Y, Tsvankin I (2006) Plane-wave propagation in attenuative transversely isotropic media. Geophysics 71(2):T17–T30. https://doi.org/10.1190/1.2187792